RSC Advances

PAPER

View Article Online
View Journal | View Issue

Cite this: *RSC Adv.*, 2016, **6**, 75315

N,*N*-Bis-(dimethylfluorosilylmethyl)amides of *N*-organosulfonylproline and sarcosine: synthesis, structure, stereodynamic behaviour and *in silico* studies†

Alexey A. Nikolin,*[a] Eugenia P. Kramarova,[a] Alexander G. Shipov,[a] Yuri I. Baukov,[a] Vadim V. Negrebetsky,[a] Dmitry E. Arkhipov,[b] Alexander A. Korlyukov,[b] Alexey A. Lagunin,[cd] Sergey Yu. Bylikin,[e] Alan R. Bassindale[e] and Peter G. Taylor[e]

Received 3rd June 2016
Accepted 22nd July 2016

DOI: 10.1039/c6ra14450k

www.rsc.org/advances

(O→Si)-Chelate difluorides $R_3R_2NCH(R_1)C(O)N(CH_2SiMe_2F)_2$ (**9a–c**, $R_1R_2 = (CH_2)_3$, R_3 = Ms (a), Ts (b); R_1 = H, R_2 = Me, R_3 = Ms (c)), containing one penta- and one tetracoordinate silicon atoms were synthesized by silylmethylation of amides $R_3R_2NCH(R_1)C(O)NH_2$, subsequent hydrolysis of unstable intermediates $R_3R_2NCH(R_1)C(O)N(CH_2SiMe_2Cl)_2$ (**7a–c**) into 4-acyl-2,6-disilamorpholines $R_3R_2NCH(R_1)C(O)N(CH_2SiMe_2O)_2$ (**8a–c**) and the reaction of the latter compounds with $BF_3{\cdot}Et_2O$. The structures of disilamorpholines **8a**,**c** and difluoride **9a** were confirmed by an X-ray diffraction study. According to the IR and NMR data, the O→Si coordination in solutions of these compounds was weaker than that in the solid state due to effective solvation of the Si–F bond. A permutational isomerisation involving an exchange of equatorial Me groups at the pentacoordinate Si atom in complexes **9a–c** was detected, and its activational parameters were determined by ^{1}H DNMR. *In silico* estimation of possible pharmacological effects and acute rat toxicity by PASS Online and GUSAR Online services showed a potential for their further pharmacological study.

Introduction

Hypercoordinate silicon compounds are the focus of intense research due to the diversity of their structures, chemical properties,[1] stereodynamic behaviour[2] and practical use in stereoselective synthesis[3] and medical diagnostics.[4] In recent years a large number of new types of pentacoordinate silicon compounds have been synthesized, including complexes with five different atoms in the silicon environment, compounds with SiO_5, SiS_2N_2C, SiS_2O_2C, SiN_4X (X = S, Se, Te) skeletons and others.[5]

At the same time, certain classes of organosilanes containing both penta- and tetracoordinate silicon atoms in the same molecule remain virtually unknown. Among these compounds are *N*,*N*-bis(dimethylhalogenosilylmethyl)amides, where two silicon centres compete for a single carbonyl group. One of the Si atoms in these amides extends its coordination number to five and forms an (O→Si)-chelate ring while another Si atom remains tetracoordinate. Up to date, very few examples of such compounds have been reported,[6] with the structures of only four complexes (**1**,[6b] **2**,[6b] **3** (ref. 6*e*) and **4** (ref. 6*e*)) determined by X-ray method.

Since each of the two silicon atoms in dihalides **1–4** can potentially form a coordination bond with the carbonyl group, these compounds are particularly interesting as models for studying stereodynamic processes in solutions (such as alternating coordination or permutational isomerisation), pathways of S_N2–Si reactions, relative contributions of the silicon centres to O→Si coordination and the effects of such coordination on the reactivity of $Si^{IV}Me_2Hal$ and $Si^{V}Me_2Hal$ groups within a single molecule.

Earlier we described (O→Si)-monochelate fluorosilanes RSO_2-Pro-N(Me)CH_2SiMe_2F (**5**), containing an electron-withdrawing organosulfonyl group at the nitrogen atom of the amino acid fragment.[7] In the present work, we report the synthesis, structures and stereodynamic behaviour of dinuclear fluorosilyl derivatives of proline and sarcosine $R_3R_2NCH(R_1)C(O)N(CH_2SiMe_2F)_2$ (**9**), synthesised by bis-silylmethylation of *N*-organosulfonyl-(*S*)-proline

[a]*Department of Chemistry, N.I. Pirogov Russian National Research Medical University, Ostrovityanov St. 1, Moscow 117997, Russian Federation. E-mail: nikson1111@yahoo.com*

[b]*A. N. Nesmeyanov's Institute of Organoelement Compounds, RAS, Vavilova St. 28, 119991 Moscow, Russian Federation*

[c]*Department of Bioinformatics, N.I. Pirogov Russian National Research Medical University, Ostrovityanov St. 1, Moscow 117997, Russian Federation*

[d]*Institute of Biomedical Chemistry, Pogodinskaya Str., 10/8, Moscow, 119121, Russian Federation*

[e]*Department of Chemistry, Open University, Walton Hall, Milton Keynes, MK7 6AA, UK*

† Electronic supplementary information (ESI) available. CCDC 1059570–1059573. For ESI and crystallographic data in CIF or other electronic format see DOI: 10.1039/c6ra14450k

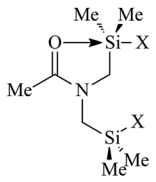

X = F (**1**), Cl (**2**)

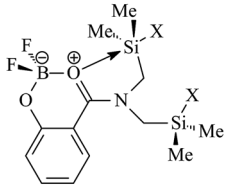

X = F (**3**), Cl (**4**)

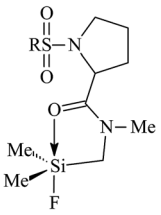

RSO_2 = R = Me, Ph, 4-MeC_6H_4, 4-ClC_6H_4, 4-BrC_6H_4 or 4-$NO_2C_6H_4$. (**5**)

and *N*-mesylsarcosine amides $R_3R_2NCH(R_1)C(O)NH_2$ (**6**) *via* unstable dichlorides $R_3R_2NCH(R_1)C(O)N(CH_2SiMe_2Cl)_2$ (7) and isolable *N*-substituted 2,6-disilamorpholines $R_3R_2NCH(R_1)C(O)N(CH_2SiMe_2O)_2$ (**8**).

Discussion of the results

Synthesis of disilamorpholines

Disilamorpholines **8** were prepared by the general synthetic approach developed by us for various silacyclanes.[6d,e,8] The starting compounds, primary amides **6**, were silylmethylated by a mixture of chloro(chloromethyl)dimethylsilane and hexamethyldisilazane with subsequent hydrolysis of unstable dichlorides **7** into target 4-acyl-2,6-disilamorpholines **8** (Scheme 1).

Mesyl and tosyl derivatives of (*S*)-proline, Ms-Pro-N$(CH_2SiMe_2)_2$O (**8a**) and Ts-Pro-N$(CH_2SiMe_2)_2$O (**8b**), and mesyl derivative of sarcosine, MsN(Me)$CH_2C(O)N(CH_2SiMe_2)_2O$ (**8c**), were obtained by one-pot syntheses with yields of 75, 78 and 80%, respectively. The composition and structures of compounds **8** were confirmed by the elemental analysis, IR and multinuclear (^{1}H, ^{13}C, ^{29}Si and CP/MAS ^{29}Si) NMR spectroscopy. The structures of compounds **8a** and **8c** were also determined by X-ray method (see below).

The formation of hydrolytically unstable dichloride **7a** was detected by IR spectroscopy. When a mixture of amide **6a** with three equivalents of $ClCH_2SiMe_2Cl$ and one equivalent of $(Me_3Si)_2NH$ was refluxed in benzene or toluene, the absorption of the NCO fragment in **6a** was gradually replaced by two absorptions (at 1590 and 1505 cm^{-1}) of the same fragment in **7a**, which was typical O→Si chelates of pentacoordinate silicon.[6b,9] IR spectra of all 4-acyl-2,6-disilamorpholines **8a–c** showed a strong absorption of the NCO fragment at 1630 cm^{-1}.

In the ^{1}H NMR spectra of chiral proline derivatives **8a**,**b**, the signals of two $SiMe_2$ groups appear as four singlets.

The ^{29}Si NMR spectra of disilamorpholines **8a–c** in solutions contain two signals at approximately 8 and 10 ppm, which are almost independent of the amino acid or *N*-substituent nature. The same chemical shifts of ^{29}Si are observed in the solid-state CP/MAS spectra of these compounds (see Experimental section). Therefore, the solvation of tetracoordinate silicon atoms has no noticeable effect on their chemical shifts.

The above data suggest that both silicon atoms in compounds **8a–c** are tetracoordinate.[6c] Similar to the double set of signals of $SiMe_2$ groups in ^{1}H NMR spectra, the presence of two signals in ^{29}Si NMR spectra of these compounds is probably caused by the hindered amide rotation.

Synthesis of difluorides

In contrast to hydrolytically labile Si–Cl bonds in pentacoordinate dichlorides **7a–c**, the Si–F bonds in their difluoro analogues **9a–c** were expected to be more stable. (O→Si)-Chelate *N*′,*N*′-bis(dimethylfluorosilylmethyl)-*N*-organosulfonyl-(*S*)-prolinamides (**9a**,**b**) and *N*′,*N*′-bis(dimethylfluorosilylmethyl)-*N*-mesylsarcosinamide (**9c**) were prepared by the reaction of disilamorpholines **8a–c** with $BF_3 \cdot Et_2O$ in acetonitrile (Scheme 2).

The composition and structure of difluorides **9a–c** were determined by the elemental analysis, IR and multinuclear (^{1}H,

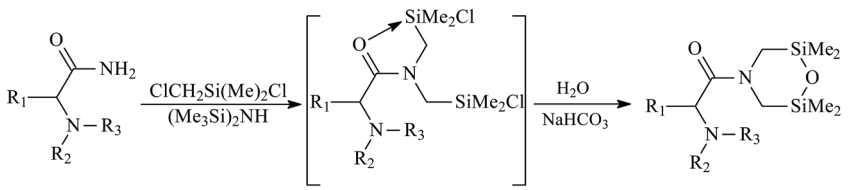

6a–c **7a–c** **8a–c**

(**a**) $R_1R_2 = (CH_2)_3$, R_3 = Ms; (**b**) $R_1R_2 = (CH_2)_3$, R_3 = Ts; (**c**) R_1 = H, R_2 = Me, R_3 = Ms

Scheme 1

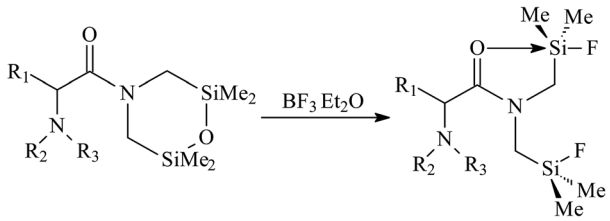

8a–c **9a–c**

(**a**) $R_1R_2 = (CH_2)_3$, R_3 = Ms; (**b**) $R_1R_2 = (CH_2)_3$, R_3 = Ts; (**c**) R_1 = H, R_2 = Me, R_3 = Ms

Scheme 2

^{13}C and ^{29}Si) NMR spectroscopy. The coordination states of both silicon atoms in compound **9a** in the solid state was further confirmed by X-ray single-crystal study (see below) and ^{29}Si CP/MAS NMR.

Multinuclear NMR spectroscopy

^1H NMR spectra of difluorides **9a–c** contain two signals of the $SiMe_2$ groups in the upfield region. These signals can be attributed to specific $SiMe_2$ groups using Bruker 2D pulse sequence {^1H-^{29}Si}HMBS. For example, the cross-peaks in the 2D spectrum of **9b** (Fig. 1) indicate that the upfield signal of $SiMe_2$ protons corresponds to the signal of pentacoordinate ^{29}Si at −20 ppm while the downfield signal of $SiMe_2$ protons corresponds to the signal of tetracoordinate ^{29}Si at +30 ppm.[2b,c]

Direct spin–spin coupling constants $^1J_{SiF}$ in NMR spectra of compounds **9** for tetracoordinate silicon (230–260 Hz) were generally lower than those for pentacoordinate silicon (*ca.* 280 Hz; see Experimental section). Such difference, observed both in solutions and solid state, reflected the weakening of the Si–F bond at Si^V in comparison with Si^{IV} (see X-ray data for **9a**).[2b,c] For the same reason, the spin–spin coupling constant $^3J_{HF}$ was observed at ambient temperature only for the $Si^{IV}Me_2$ group but not for the Si^VMe_2 group. Finally, the weakening of the Si^V–F bonds affected the $^2J_{CF}$ constants in ^{13}C NMR spectra: the observed spin–spin coupling frequencies at Si^V centres (10–15 Hz) were significantly lower than those at the Si^{IV} centres (*ca.* 30 Hz).

Intramolecular O→Si coordination in complexes **9** in solutions was further confirmed by the down field shift of the C=O

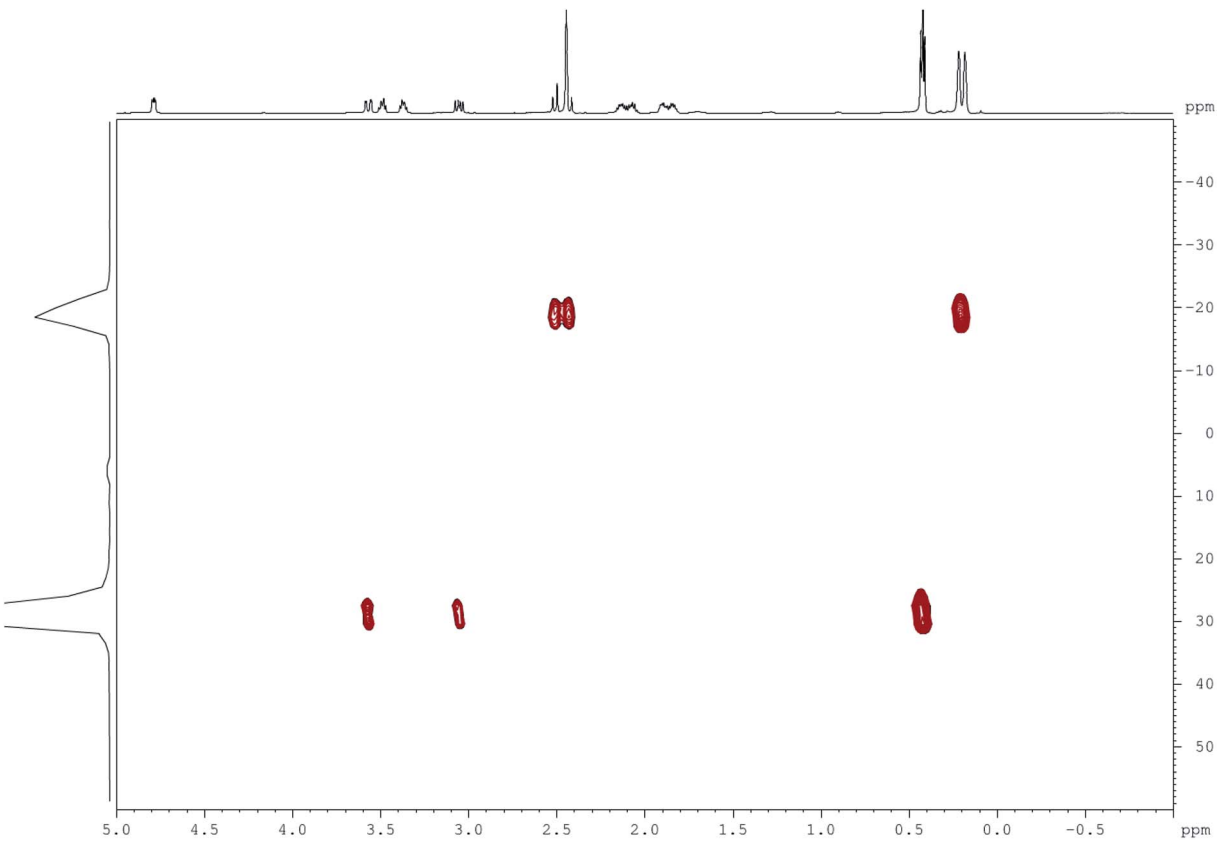

Fig. 1 Two-dimensional NMR spectrum of **9b** (Bruker {^1H-^{29}Si}HMBS, $CDCl_3$, 600 MHz).

signal in their ^{13}C NMR spectra. The characteristic patterns of $Si^{V}(CH_3)_2$ and NCH_2Si^{V} signals in ^{1}H NMR spectra of difluorides **9a**,**b** (two singlets of equal intensity and an AB-system quartet, respectively) indicated the presence of a chiral carbon atom in their molecules.

The ^{29}Si signals in solid-state NMR spectra of compounds **9** had greater upfield shifts (*ca.* −40 ppm) than the same signals in solutions (*ca.* −10 ppm). Similar effect was observed for monofluorides **5** and was probably caused by effective solvation of pentacoordinate silicon.[7a]

Using the difference between the observed chemical shifts of a Si^{V} atom and the typical chemical shift of a Si^{IV} atom (*ca.* 30 ppm), the *coordination contribution* ($-\Delta\delta = \delta Si^{V} - \delta Si^{IV}$)[2a] in difluorides **9** can be estimated to be approximately 50 ppm. The comparison of this value to coordination contributions in chlorosilanes RSO_2-Pro-N(Me)CH_2SiMe_2Cl (70–75 ppm), silyloxonium halides [R-Pro-N(Me)$CH_2SiMe_2OH_2$]X (R = AlkSO_2, ArSO_2, Ac; X = Cl, Br) (70–80 ppm)[10] and theoretical data for monofluorosilanes **5** (ref. 7*b*) and MeC(O)N(Me)CH_2SiMe_2F[11] (same as above) indicates a relatively weak coordination in difluorides **9**.

All difluorides have two signals in their ^{19}F NMR spectra: one at approximately −159 ppm and another at −119 ÷ −125 ppm. According to literature data, these signals belong to $Si^{IV}Me_2F$ and $Si^{V}Me_2F$ groups, respectively.[2b,c]

Variable-temperature ^{1}H, ^{19}F and ^{29}Si NMR studies

The strength of intramolecular coordination in monochelates of pentacoordinate silicon strongly depends on the nature of the substituent X (Scheme 3; see[2c,7a] and references therein).

In the case of compounds with the $OSiC_3X$ coordination set and X = Hal or OTf, structures **A** and **B** are typical for fluorides, **C** for chlorides, **D** for bromides, and **E** for iodides and triflates.

To study the temperature effects on the coordination set structure in difluorides **9a–c**, the temperature-dependent ^{1}H, ^{19}F and ^{29}Si NMR spectra of these compounds in $CDCl_3$ were obtained. The decrease in temperature from +20 to −60 °C led to reversible downfield shifts of ^{1}H and ^{19}F signals (by *ca.* 0.03 and 3–4 ppm, respectively) of the $Si^{V}Me_2F$ group. At the same time, the chemical shift of ^{19}F in the $Si^{IV}Me_2F$ group was not affected by the temperature. Such behaviour of ^{1}H and ^{19}F signals suggests an increased contribution of form **B** (Scheme 3) at low temperatures.

Similar to monofluorosilanes,[7a] the increase in temperature to +60 °C caused very small reversible broadening of the $SiMe_2$ and NCH_2 signals in ^{1}H NMR spectra of difluorides **9a–c**. Such broadening was indicative of a permutational isomerisation at the Si^{V} coordination set of these compounds.

The activation parameters of the permutation were calculated by a ^{1}H DNMR method using a full line-shape analysis of the signals. For all studied compounds, the stereodynamic processes in $CDCl_3$ were characterised by a narrow range of activation energies (~24 kcal mol^{-1} or greater) and high negative values of the entropy of activation (*ca.* ~ −20 cal mol^{-1} K^{-1}). These values were very similar to the activation parameters of *N*-(dimethylfluorosilylmethyl)- and *N*-[fluoro(methyl)(phenyl)silylmethyl]amides and -lactams,[2a,12–15] as well as RSO_2-Pro-N(Me)CH_2SiMe_2F (**5**),[6a] where R = Me, Ph, 4-MeC_6H_4, 4-ClC_6H_4, 4-BrC_6H_4 or 4-$NO_2C_6H_4$.

XRD studies

Disilamorpholine **8a** (Fig. 2) crystallizes in two polymorph modifications (**8a** and **8a′**).

The orthorhombic ($P2_12_12_1$) crystals **8a** were obtained from a heptane–benzene mixture with a molar ratio of 3 : 1, whereas

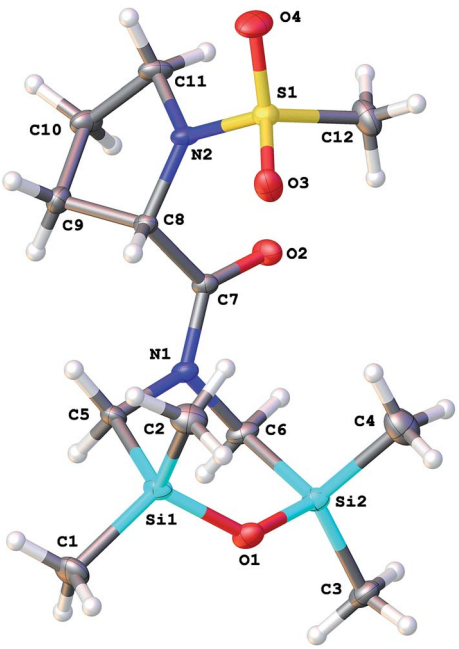

Fig. 2 Molecular structure of **8a** with thermal ellipsoids shown at the 50% probability level.

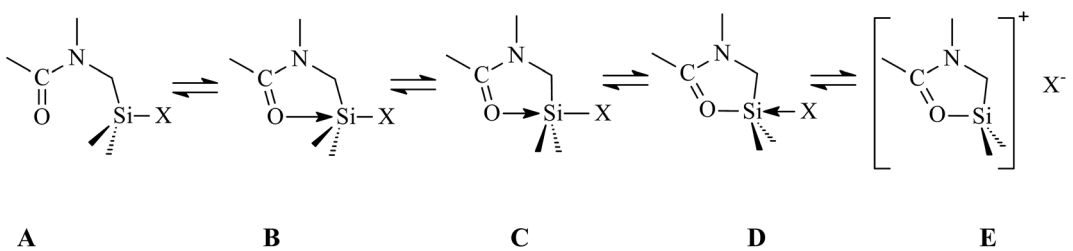

Scheme 3

monoclinic ($P2_1$) crystals **8a′** were obtained from ethanol. There are two crystallographically independent molecules in the asymmetric unit of **8a**; its volume is 3.84 times larger than that of **8a′**, because the cell **8a′** contains a void of about 40 Å^3. The structure of the 2,6-disilamorpholine fragment in compounds **8a**, **8a′** and **8c** (Fig. 3) is analogous to the previously published five structures (CSD refcodes:[16] QOMTAN, QOMTER, XATQIT, XULNAT, XULNEX).

The mesyl group and 2,6-disilamorpholine fragment have *syn*-conformation relative to the proline ring: the corresponding torsion angles C8–N2–S1–C12 and C20–N4–S2–C24 in **8a** are 95.3(2)° and 88.8(2)° for two crystallographically independent molecules, respectively, and the torsion angle C8–N2–S1–C12 in **8a′** is 94.7(5)°.

An asymmetric unit of difluoride **9a** contains two crystallographically independent molecules, which differ by mutual orientation of the proline moiety and Me_2FSiCH_2 group relative to the chelate ring. In the case of *syn*-conformation, the interatomic distance S1···Si2 is 5.387(1) Å, whereas for *anti*-configuration the distance S2···Si4 is 6.340(1) Å. In **9a** (Fig. 4), one of the silicon atoms is pentacoordinated, and its coordination polyhedron is a distorted trigonal bipyramid (axial angles O1–Si1–F1 and O4–Si3–F3 are 172.1(1)° and 171.9(1)°, the deviations of Si1 and Si3 atoms from the planes of equatorial substituents toward fluorine atoms are 0.167(1) Å and 0.176(1) Å for two crystallographically independent molecules, respectively).

The structures of coordination polyhedra of Si1 and Si2 atoms in **9a** are noticeably different from those in the series of (O→Si)-chelate *N′*-(dimethylfluorosilylmethyl)-*N′*-methyl-*N*-(organosulfonyl)prolinamides,[7a] complexes **1** (ref. 6*d*) and **3** (ref. 6*e*) (selected bond lengths are given in Table 1).

The structure of **3** differs significantly from other difluorides due to the coordination of amide oxygen atom with the difluoroboron group while the coordination with the silicon atom is very weak. Thus, the axial Si–O bonds are shortened by 0.07–0.17 Å, and Si^V–F bonds lengthened by 0.02–0.04 Å compared to similar bonds in prolinamide derivatives and difluoride **1**. The Si^{IV}–F bonds are lengthened by 0.05–0.10 Å in comparison with similar bonds in difluorides **1** and **3**. Atoms Si2 and Si4 are not coordinated by any oxygen atoms, with the shortest intermolecular contact Si4···O2 of 3.538(1) Å.

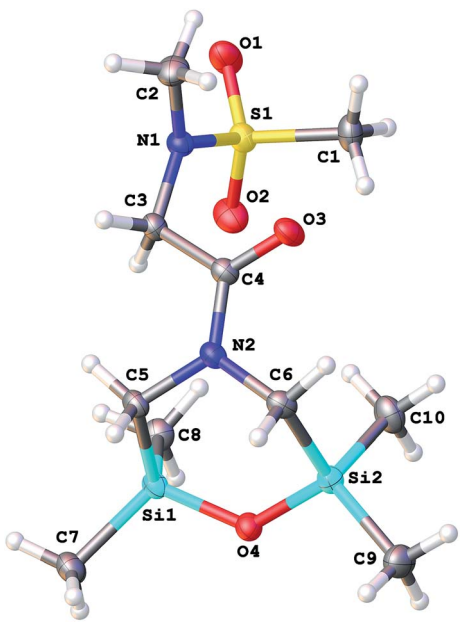

Fig. 3 Molecular structure of **8c** with thermal ellipsoids shown at the 50% probability level.

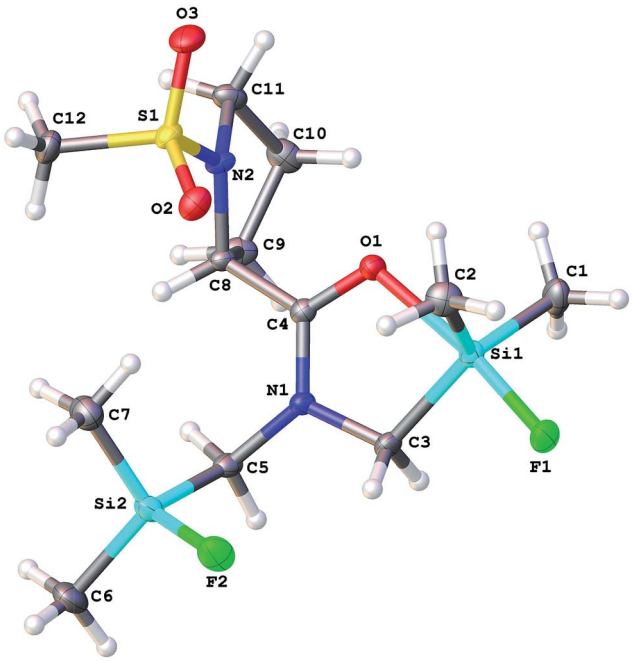

Fig. 4 Molecular structure of **9a** with thermal ellipsoids shown at the 50% probability level.

Quantum-chemical studies of the permutational isomerization

To test the applicability of the mechanism (Scheme 4) previously suggested for the permutational isomerisation of *N*-(dimethylfluorosilylmethyl)amides[1] to *N*,*N*-bis-(dimethylfluorosilylmethyl)amides, we carried out quantum chemical studies of molecule **9a**.

At higher temperatures, the equilibrium **B** ⇌ **A** (Schemes 3 and 4) shifts towards the tetracoordinate topomer **A**. The nucleophilic attack at the Si atom by a fluoride anion (F^{*-}) produces pentacoordinate difluoride **G**, which subsequently loses the F^- anion and forms tetracoordinate intermediate **H**. The rotation around the Si–CH_2 bond produces topomer **A′** and

Table 1 Selected bond lengths for structures **9a**, **1**, **3** and prolinamide derivatives

	9a (mean values)	**1** (ref. 6*d*)	**3** (ref. 6*e*)	Monofluorides[7a]
Si^{IV}–F	1.613(1)	1.603	1.608	—
Si^{V}–F	1.693(1)	1.668	1.620	1.651–1.671
Si···O	2.062(1)	2.187	2.918	2.131–2.220

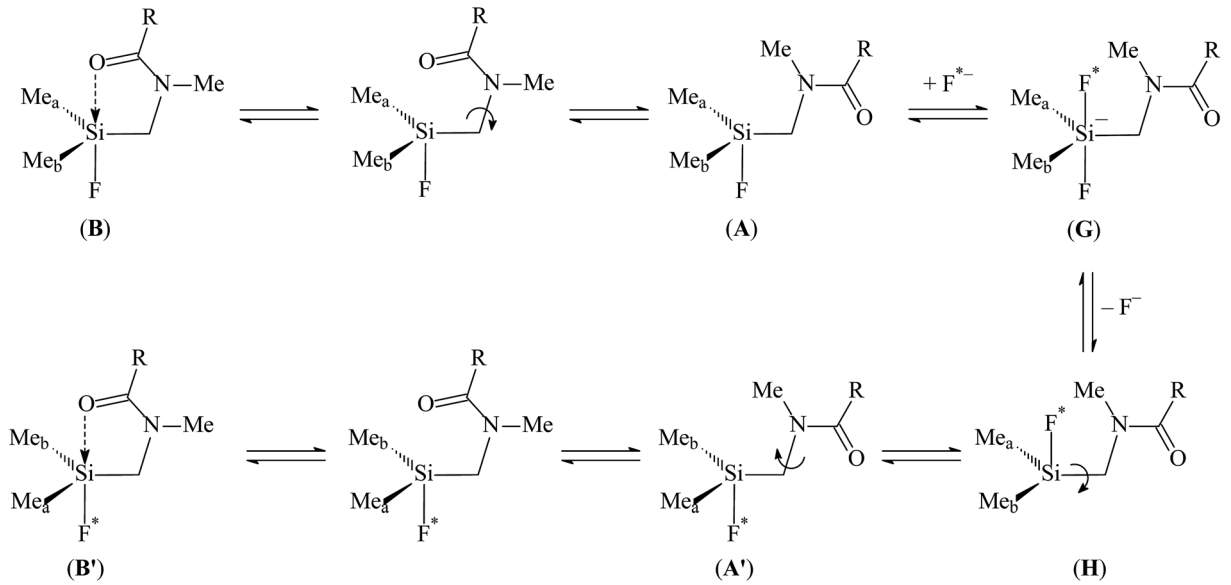

Scheme 4

finally complex **B′** with inverted orientation of the methyl groups at silicon.

According to our previous study, the external fluorine anion can attack tetracoordinated silicon, and the dissociation energy of resulting Si–F bond in gas phase is equal to ~90 kcal mol^{-1}. Solvation of the F$^-$ anion leads to significant decrease of the Si–F dissociation energy. It is reasonable to assume that similar processes can occur in solution of **9a** in $CDCl_3$. Due to the presence of two dimethylfluorosilylmethyl and one bulky tosyl groups, the silicon atoms seems to be less accessible for nucleophilic attack as compared to *N*-(dimethylfluorosilylmethyl) amides, where only one dimethylfluorosilylmethyl group is present. Hence, the stereodynamic processes in solution of **9a** can be more complex as compared to *N*-(dimethylfluorosilylmethyl)amides.[7a]

An alternative mechanism can involve the carbonyl group migration from one dimethylfluorosilyl to another (similarly to derivatives urea[17]) (Scheme 5).

In any case, the cleavage of the Si–O coordination bond and the certain conformational changes are necessary to the transfer the carbonyl oxygen atom from one dimethylfluorosilylmethyl to another. Thus, the detailed inspection of these processes can be very useful for understanding the nature of permutational isomerisation in the solution of **9a**.

Quantum-chemical calculations of **9a** were carried out using Gaussian 03W program.[18] Hybrid PBE0 functional and 6-311G(d,p) basis set were utilized for structure optimization, hessian calculations, relaxed potential energy scans and transition state search. To account for the effect of nonspecific solvation, the PCM model was applied (the value of dielectric constant corresponded to chloroform). All calculations was performed with tight optimization criteria (Opt = tight) and precise grid for computation of two-electron integrals (Int(Grid = Ultrafine)). Molecular graphics was drawn with ChemCraft program.[19] General views of calculated structures, atomic coordinates and total energies can be found in ESI.†

Analysis of potential energy surface for **9a** in its isolated molecule and $CDCl_3$ (PCM calculation) has shown that the presence of two conformational isomers correspond to the cyclic structures (where the Si–O coordination bond is present) and two other conformers belong are acyclic (Si–O coordination bond is absent). According to quantum chemical calculations, the influence of dielectric continuum used in PCM model leads to significant changes in molecular structure of **9a**. The most noticeable change is the decrease of Si1···O1 distance from 2.36–2.37 to 2.25 Å. Cyclic conformers are more favourable as compared to the acyclic conformers. The difference between two isolated most stable cyclic and acyclic structures is 2.51 kcal mol^{-1}. The use of PCM model for the description of solvation increases this difference to 4.37 kcal mol^{-1}, which is in good agreement with our earlier calculations.[7a] All cyclic conformers can be characterized by the same geometry of coordination

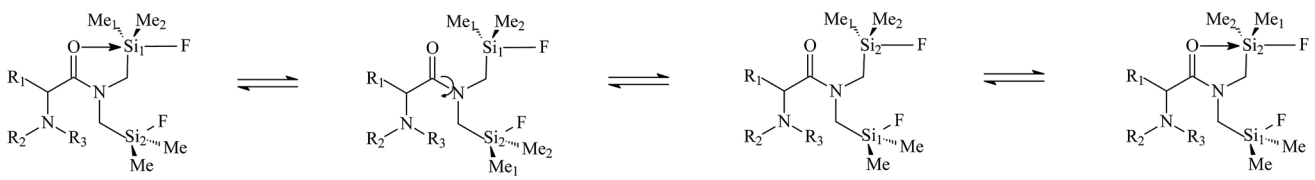

Scheme 5

polyhedra of silicon atoms, so their ^{19}F and ^{29}Si chemical shifts should be very close.

Other differences are related to mutual orientation of *N*-organosulfonyl and dimethylfluorosilyl groups. In isolated cyclic and acyclic forms of **9a**, these fragments are much closer to each other than in the solution. In two conformers (**9a**-cyclic2 and **9a**-acyclic2, Fig. 5S and 6S, see ESI†), the Si2⋯O2 distances between one of the $SiMe_2F$ groups and the oxygen atom of the sulfonyl group are 3.698 and 3.720 Å, respectively. The optimization of these conformers in terms of PCM model (**9a**-cyclic2-$CDCl_3$ and **9a**-acyclic2-$CDCl_3$, Fig. 7S and 8S†) increases the separation of the above fragments (the Si2⋯O2 distances become 4.533 and 3.962 Å). Conformers **9a**-cyclic and **9a**-acyclic (Fig. 1S and 2S†) are stabilized by weak C–H⋯O bonds between sulfonyl and methyl groups, so the Si2⋯O2 distances are 3.724 and 4.450 Å. Again, the application of PCM model increases Si2⋯O2 distances to 4.292 and 4.376 Å (**9a**-cyclic-$CDCl_3$ and **9a**-acyclic-$CDCl_3$, Fig. 3S and 4S†). Thus, the effect of nonspecific solvation prevents the formation of Si2⋯O2 interactions, so the permutational isomerisation involving the sulfonyl group is unlikely to take place.

The information about the barrier of rotation around Si1–C3 and N1–C4 bonds can be useful to understand the mechanism of permutational isomerisation of **9a**. These barriers were calculated by the relaxed potential energy surface scan of CNCO and F1Si1C3N1 torsion angles (the plots of the energy *vs.* scan coordinate are placed in ESI (Fig. 9S and 10S†)). The value of the rotation barrier around the Si1–C3 bond in isolated molecule **9a** is approximately 7 kcal mol^{-1} (Fig. 9S†), so the rotation around the Si–C bond is possible despite the presence of an Si1–O1 coordination bond. In solution, the value of this barrier is even lower than that in isolated molecule (~5.1 kcal mol^{-1}). It is not surprising that the rotation around the N1–C4 bond is less favourable than the rotation around the Si1–C3 bond. Firstly, the N1–C3 bond is intermediate between ordinary and double (Table 2). Secondly, the rotation around the N1–C3 bond is attributed to the formation and cleavage of Si1–O1 and Si2–O1 coordination bonds. Our calculation gave the values of 26.3 kcal mol^{-1} for isolated molecule **9a** and 24.8 kcal mol^{-1} for its solution in chloroform (Fig. 10S†). These values are very close to the permutational barriers measured for **9a–c** by ^{19}F DNMR study. Thus, the internal rotation can be responsible for the permutational isomerisation of **9a**. Additional justification for this assumption was obtained by the localization of transition states (Fig. 11S and 12S†). The modes of negative vibrations (−67.0 and −62.8 cm^{-1} for isolated molecule and $CDCl_3$ solution, respectively) correspond to the rotation around the N1–C4 bond and formation/dissociation of Si–O coordination bonds. The difference between energies of the most favourable cyclic conformers and transition state is 28.4 and 29.3 kcal mol^{-1} for isolated molecules and solution of **9a**, respectively. These values are in agreement with the results of DNMR study. At the same time, the ΔS value calculated as the difference between the transition state and cyclic isomer is ~−2 kcal mol^{-1} K^{-1}, which is much lower than the experimental value. In our opinion, this difference can be explained by specific solvation (for instance, H-bonds between $CDCl_3$ and carbonyl or sulfonyl groups, which can be responsible for stabilization of particular conformers).

Table 2 Calculated bond distances and angles in conformers of **9a**

Conformer	Si1⋯O1	Si2⋯O2	Si1–F1	Si2–F2	O1Si1F1
9a-cyclic	2.368	4.450	1.665	1.632	169.20
9a-acyclic	3.130	3.724	1.638	1.646	79.69
9a-cyclic-$CDCl_3$	2.248	4.533	1.686	1.640	170.25
9a-acyclic-$CDCl_3$	3.222	3.962	1.652	1.644	78.82
9a-cyclic2	2.356	3.698	1.667	1.637	168.96
9a-acyclic2	2.984	3.720	1.637	1.639	76.09
9a-cyclic2-$CDCl_3$	2.250	4.292	1.686	1.643	169.97
9a-acyclic2-$CDCl_3$	3.175	4.376	1.644	1.644	77.90
9a-ts	4.828	3.969	1.638	1.637	112.44
9a-ts-$CDCl_3$	4.947	3.777	1.645	1.648	115.07

In silico estimation of possible pharmacological applications

Possible applications of synthesized complexes were evaluated by the search for similar compounds with known activities and computational prediction of biological activity based on "structure–activity" relationships (SAR) models. Such analysis provides a reasonable basis for planning further experimental studies of biological activity.

In this study, we used the PubChem structural search for identification of equivalent and similar structures (https://pubchem.ncbi.nlm.nih.gov).[20] The similarity was assessed by the Tanimoto equation and the PubChem dictionary-based binary fingerprint analysis (https://pubchem.ncbi.nlm.nih.gov/search/help_search.html). The search results for similar compounds are shown in Table 3.

According to Table 3, the studied complexes have different similar compounds with variable known activities. No two complexes have the same most similar compound, which could indicate their similar biological potentials.

Computational prediction of biological activity for studied complexes was carried out using SAR-based online services. Possible therapeutic effects and mechanisms of action were evaluated by PASS Online[21] (http://www.way2drug.com/PASSOnline) while the LD_{50} values for acute rat toxicity were estimated by GUSAR Online[22] (http://www.way2drug.com/gusar/acutoxpredict.html). The results of these predictions are summarized in Table 4.

The prediction results suggest that synthesized compounds may possess cardiovascular and CNS properties. Low levels of predicted acute rat toxicity makes them suitable for all routes of administration.

Conclusions

New difluorides $R_3R_2NCH(R_1)C(O)N(CH_2SiMe_2F)_2$ (**9a–c**) with one pentacoordinate and one tetracoordinate silicon atoms were synthesized by silylmethylation of amides $R_3R_2NCH(R_1)C(O)NH_2$, subsequent hydrolysis of unstable intermediates $R_3R_2NCH(R_1)C(O)N(CH_2SiMe_2Cl)_2$ (**7a–c**) into 4-acyl-2,6-disilamorpholines $R_3R_2NCH(R_1)C(O)N(CH_2SiMe_2O)_2$ (**8a–c**) and the reaction of the latter compounds with $BF_3 \cdot Et_2O$.

Table 3 The search results for similar compounds in PubChem[a]

ID	Hits (probability)	The most similar compound with data on patents or activity
8a	0 (90%); 161 (80%)	*N*-[(3*S*)-1-Methyl-2-oxopiperidin-3-yl]-*N*-(2-oxopropyl)methanesulfonamide (CID 58869395) Patent description: sulfonylaminovalerolactams and derivatives thereof as factor Xa inhibitors
8b	216 (90%)	4,4′-Ethylenebis(1-methyl-2,6-piperazinedione) (CID 97592) Patent description: novel drug targets to overcome *de novo* drug-resistance in multiple myeloma; method of reducing amyloid-beta peptide levels using a bisdioxopiperazine; abatement process for contaminants; bis-dioxopiperazines and their use as protection agents bis-dioxopiperazines and their use as protection agents Known activity: small molecule inhibitors of FGF22-mediated excitatory synaptogenesis & epilepsy measured in biochemical system using RT-PCR – 7012-01_Inhibitor_SinglePoint_HTS_Activity
8c	0 (90%); 19 (80%)	2-(4-Acetylpiperazin-1-yl)-*N*-methylsulfonylacetamide (CID 89504348) Patent description: dual-acting antihypertensive agents having angiotensin II type receptor antagonist activity and neprilysin-inhibition activity
9a	0 (90%); 74 (80%)	(1) *N*-(4-Amino-5-oxo-5-pyrrolidin-1-ylpentyl) methanesulfonamide (CID 17960593) Patent description: alpha-amino acid sulphonyl compounds (2) (2*S*)-1-[2-[Methyl(methylsulfonyl)amino] ethyl]pyrrolidine-2-carboxamide (CID 57572120) Patent description: quinolinone compounds as 5-HT4 receptor agonists
9b	59 (90%)	Azepan-1-yl-[1-(4-methylphenyl) sulfonylpyrrolidin-2-yl]methanone (CID 2964486) Known activity: active in HTS assay for activators of cytochrome P450 2A9
9c	0 (90%); 10 (80%)	*N*,*N*-Dimethyl-2-[methyl(methylsulfonyl)amino] acetamide (CID 57682568) Patent description: HIV integrase inhibitors

[a] Hits – number of similar compounds (≥90% or ≥ 80% Tanimoto index); CID – PubChem Compound ID.

According to IR and NMR data, the O→Si coordination in solutions of these compounds was weaker than in the solid state due to effective solvation of the Si–F bond. The absence of spin–spin coupling constants $^3J_{HF}$ of the methyl groups at Si^V and their retention at Si^{IV} indicates a significant weakening of the Si–F bond at pentacoordinate silicon, which favours its ionization. Based on *in silica* analysis, the synthesized compounds show a potential for pharmacological studies.

Experimental section

IR-spectra of compounds in solution and in the solid state were recorded on a Bruker Tensor-27 spectrometer using KBr cells and an APR element, respectively. ^{1}H, ^{13}C and ^{19}F NMR spectra in $CDCl_3$ and DMSO-d_6 were recorded on a Bruker Avance II 300 (^{1}H, 300 MHz; ^{13}C, 75.6 MHz; ^{19}F, 282.2 MHz) and Jeol JNM-EX400 (^{1}H, 400 MHz; ^{13}C, 100.6 MHz; ^{19}F, 376.3 MHz) instruments using standard pulse sequences. ^{29}Si NMR spectra were recorded using the ^{1}H-^{29}Si HSQC pulse sequence supplied with the Bruker Avance II 600 instrument.[23] The ^{1}H, ^{13}C, ^{29}Si chemical shifts were measured using Me_4Si as internal reference. The ^{19}F chemical shifts were measured using BF_3 as external reference. Negative values are to high field. ^{29}Si NMR CP/MAS spectra in the solid state were recorded on a Jeol JNM-EX-400 instrument using 5 mm zirconia rotors and a Doty probe.

The temperature calibration of the NMR spectrometers was performed by measuring the differences in chemical shifts between non-equivalent protons in methanol (−90…+30 °C)

Table 4 Prediction of therapeutic effects and mechanisms of action (PASS Online) and LD_{50} values of acute rat toxicity (GUSAR Online)[a]

ID	Top 5 predicted therapeutic effects with probability > 50%	Top 5 predicted mechanisms of action with probability > 50%	Predicted LD_{50} values in mg kg^{-1}, type of administration, class of toxicity
8a	Not predicted	Acetylcholine neuromuscular blocking agent	IP – out of AD, 127, IV, 4 class, 904, PO, 4 class, SC – out of AD
8b	Not predicted	Acetylcholine neuromuscular blocking agent	IP – out of AD, 96, IV, 4 class, 1270, PO, 4 class, SC – out of AD
8c	Spasmolytic	Acetylcholine neuromuscular blocking agent, anaphylatoxin receptor antagonist	IP – out of AD, 156, IV, 4 class, 453, PO, 4 class, 250, SC, 4 class
9a	Antianginal, multiple sclerosis treatment, antiparkinsonian, neurodegenerative diseases treatment	Phosphatidylinositol 3-kinase C2beta inhibitor, RANTES antagonist, insulin growth factor agonist, insulin like growth factor 1 agonist	IP – out of AD, 80, IV, 4 class, PO – out of AD, 487, SC, 4 class
9b	Antianginal, cardiovascular analeptic, multiple sclerosis treatment, cell adhesion molecule inhibitor	Integrin alpha2 antagonist, calmodulin antagonist, nicotinic alpha4beta4 receptor agonist	IP – out of AD, 101, IV, 4 class, PO – out of AD, SC – out of AD
9c	Antianginal	Anaphylatoxin receptor antagonist, phospholipid-translocating ATPase inhibitor, 2-haloacid dehalogenase inhibitor, glycosylphosphatidylinositol phospholipase D inhibitor, NADPH peroxidase inhibitor	IP – out of AD, 130, IV, 4 class, PO – out of AD, 225, SC, 4 class

[a] IP – intraperitoneal route of administration; IV – intravenous route of administration; PO – oral route of administration; SC – subcutaneous route of administration; out of AD – compound is out of applicability domain of QSAR models.

and ethyleneglycol (+30…+85 °C).[24] The activational parameters of the permutational isomerisation were calculated using DNMR-SIM software[25] and a modified Eyring equation.[26] In each case, at least twelve temperature points were obtained to achieve a correlation coefficient of 0.997–0.999.

Chloro(chloromethyl)dimethylsilane, (*S*)-proline hydrochloride, sarcosine and all solvents were purchased from Acros and Sigma-Aldrich. Ethyl esters of *N*-mesyl-(*S*)-proline and *N*-tosyl-(*S*)-proline were synthesised as described earlier.[10]

Ethyl-*N*-mesyl-*N*-methylglycinate

Thionyl chloride (83.3 g, 0.27 mol) was added dropwise to a solution of *N*-methylglycine (44.5 g, 0.50 mol) in absolute ethanol (200 mL). The mixture was refluxed for 5 h, then the volatiles were removed in vacuum. The residue was suspended in an ice-cold mixture of water (20 mL) and diethyl ether (100 mL), and a solution of potassium hydroxide (28.0 g, 0.50 mol) in water (20 mL) was added over 5 min at 0 °C, followed by 250 g of anhydrous potassium carbonate. The organic layer was separated, the residue was washed with ether (2 × 50 mL), and the combined organic solutions were dried over magnesium sulfate. The solvent was removed in vacuum, and the residue was distilled to afford 38.0 g (65%) of ethyl *N*-methylglycinate with b.p. 43–45 °C (12 torr) and n_D (ref. 20) 1.4105. Literature data:[27] b.p. 46 °C (12 torr), n_D (ref. 20) 1.4144.

Methanesulfonyl chloride (11.5 g, 0.10 mmol) was added dropwise to a cooled solution of ethyl-*N*-methylglycinate (11.7 g, 0.10 mol) and triethylamine (10.1 g, 0.10 mol) in diethyl ether (80 mL). The mixture was stirred at ambient temperature for 2 h, the precipitate formed was filtered off, washed with ether (15 mL), and the combined organic solutions were evaporated in vacuum. The residue was distilled to afford 13.7 g (70%) of ethyl-*N*-mesyl-*N*-methylglycinate with b.p. 144–145 °C (9 torr) and m.p. 34–35 °C. IR spectrum (KBr, ν, cm^{-1}): 1750 (C=O), 1360 and 1160 (SO_2). ^{1}H NMR spectrum ($CDCl_3$, δ, ppm (J, Hz)): 1.25 (3H, t, ^3J 7.3, CH_2CH_3); 2.77 (3H, s, CH_3N); 2.87 (3H, s, CH_3S); 4.05 (2H, s, NCH_2). ^{13}C NMR spectrum ($CDCl_3$, δ, ppm): 8.9 (CH_2CH_3); 35.3 (CH_3N); 38.1 (CH_3S); 51.4 (NCC(O)); 55.5 (CH_2CH_3); 173.9 (C=O). Found, %: C 37.08; H 6.65; N 7.11. $C_6H_{13}NO_4S$. Calculated, %: C 36.91; H 6.71; N 7.17.

N-Mesyl-(*S*)-prolinamide (6a)

Ethyl ester of *N*′-mesyl-(*S*)-proline (6.6 g, 30 mmol) was stirred with 50 mL of a 25% aqueous ammonia solution for 5 days at ambient temperature. The precipitate formed was isolated by filtration, dried in the open air and used without further purification. Yield 5.5 g (96%), m.p. 156–157 °C (from EtOH), $[\alpha]_D^{25}$ −101.3° (c 1.93, H_2O). IR spectrum (KBr, ν, cm^{-1}): 3449, 3170 (NH_2); 1619 (NCO), 1321 and 1140 (SO_2). ^{1}H NMR spectrum (DMSO-d_6, δ, ppm (J, Hz)): 1.75–2.25 (4H, m, 3,4-CH_2); 2.83 (3H, s, CH_3); 3.25–3.47 (2H, m, 5-CH_2); 3.96–4.09 (1H, m, 2-CH); 6.1 and 6.7 (2H, two broad s, NH_2). ^{13}C NMR spectrum (DMSO-d_6, δ, ppm): 22.0 (Me); 26.0 (C-4); 32.3 (C-3); 50.7 (C-5); 63.5 (C-2); 175.8 (C=O). Found, %: C 37.35; H 6.39; N 14.50. $C_6H_{12}N_2O_3S$. Calculated, %: C 37.49; H 6.29; N 14.57.

N-Tosyl-(*S*)-prolinamide (6b)

Prepared similar to **6a**. Yield 6.2 g (93%), m.p. 161–162 °C (from EtOH), $[\alpha]_D^{25}$ −134.6° (*c* 1.06, H_2O). IR spectrum (KBr, ν, cm^{-1}): 1643 (NCO), 1344, 1156 (SO_2). ^1H NMR spectrum (DMSO-d_6, δ, ppm (*J*, Hz)): 1.31–1.83 (4H, m, 3,4-CH_2); 2.43 (3H, s, CH_3); 3.11–3.22 and 3.35–3.55 (2H, m, 5-CH_2); 3.91–4.01 (1H, m, 2-CH); 5.95 and 6.71 (2H, two broad s, NH_2); 7.36 (2H, d, ^3J = 8.3, H Ar); 7.72 (2H, d, ^3J 8.3, H Ar). ^{13}C NMR spectrum (DMSO-d_6, δ, ppm): 22.0 (Me); 25.7 (C-4); 31.8 (C-3); 50.9 (C-5); 63.7 (C-2); 129.2 (C-3,5 Ar); 131.4 (C-2,6 Ar); 135.4 (C-1 Ar); 145.8 (C-4 Ar); 175.5 (C═O). Found, %: C 37.58, H 6.27, N 14.50. $C_6H_{12}N_2O_3S$. Calculated, %: C 37.49, H 6.29, N 14.57.

N-Mesyl-*N*-methylglycinamide (6c)

Prepared similar to **6a**. Yield 4.1 g (82%), m. p. 170–171 °C (EtOH). IR spectrum (KBr, ν, cm^{-1}): 3315, 3170 (NH_2); 1657 (NCO), 1320 and 1150 (SO_2). ^1H NMR spectrum (DMSO-d_6, δ, ppm (*J*, Hz)): 2.79 (3H, s, CH_3); 2.87 (3H, s, CH_3S); 3.58 and 3.71 (2H, two s, NCH_2); 5.5 and 6.1 (2H, two broad s, NH_2). ^{13}C NMR spectrum (DMSO-d_6, δ, ppm): 34.3 (CH_3N); 37.1 (CH_3S); 50.9 (NCC(O)); 174.9 (C═O). Found, %: C 29.18, H 5.92, N 16.81. $C_4H_{10}N_2O_3S$. Calculated, %: C 28.91, H 6.06, N 16.86.

2,2,6,6-Tetramethyl-4-[*N*-mesyl-(*S*)-prolinyl]-2,6-disilamorpholine (8a)

A mixture of **6a** (0.96 g, 5 mmol), hexamethyldisilazane (0.81 g, 5 mmol), chloro(chloromethyl)dimethylsilane (2.15 g, 15 mmol) and toluene (10 mL) was refluxed for 4 h, then allowed to cool down, and the precipitate formed was filtered out. The remaining solution was evaporated in vacuum, the residue was dissolved in chloroform (30 mL) and stirred with a solution of $NaHCO_3$ (0.84 g, 10 mmol) in water (10 mL) for 2 h. The organic layer was separated, the aqueous layer was extracted with chloroform (20 mL), and the combined organic solutions were evaporated in vacuum. Recrystallisation of the residue from heptane/benzene (3 : 1) mixture afforded 1.32 g (75%) of compound **8a** with m.p. 121–124 °C and $[\alpha]_D^{25}$ −55.0° (*c* 1.31, $CHCl_3$). Found, %: C 41.25, H 7.56, N 7.80, S 9.03. $C_{12}H_{26}N_2O_4SSi_2$. Calculated, %: C 41.11, H 7.48, N 7.99, S 9.15. IR spectrum (KBr, ν, cm^{-1}): 1631 s (C═O), 1325 s, 1148 s (SO_2). ^1H NMR spectrum ($CDCl_3$, δ, ppm): 0.18, 0.19, 0.21 and 0.31 (four s, 12H, $2Si(CH_3)_2$); 1.88–2.34 (m, 4H, C^3H_2 and C^4H_2 Pro); 2.7 and 3.42 (dd, 2H, NCH_2Si, $^3J_{HH}$ 15.34 Hz); 2.83 (dd, 2H, NCH_2Si, $^3J_{HH}$ 15.34 Hz); 3.01 (s, 3H, SCH_3); 3.45–3.52 and 3.56–3.63 (two m, 2H, C^5H_2 Pro); 4.80–4.87 (m, 1H, C^2H Pro). ^{13}C NMR spectrum ($CDCl_3$, δ, ppm): –0.76 ÷ 0.00 (m, $2SiMe_2$); 24.65 (^4C Pro); 30.79 (^3C Pro); 39.9 (SC); 38.1 and 40.29 (two s, NCH_2Si); 47.54 (^5C Pro); 58.92 (C^2 Pro); 169.64 (C═O). ^{29}Si NMR spectrum ($CDCl_3$, δ, ppm): 8.0, 10.5.

2,2,6,6-Tetramethyl-4-[*N*-tosyl-(*S*)-prolinyl]-2,6-disilamorpholine (8b)

Prepared similar to **8a** from 1.34 g of **6b**. Yield 1.66 g (78%) with m. p. 110–112 °C (from heptane–benzene, 10 : 1) and $[\alpha]_D^{25}$ −2.92° (*c* 1.85, $CHCl_3$). Found, %: C 50.51, H 7.24, N 6.62, S 7.45. $C_{18}H_{30}N_2O_4SSi_2$. Calculated, %: C 50.67, H 7.09, N 6.57, S 7.52. IR spectrum (KBr, ν, cm^{-1}): 1629 s (C═O), 1580 m (Ar), 1325 s, 1148 s (SO_2). ^1H NMR spectrum ($CDCl_3$, δ, ppm): 0.17, 0.21, 0.23 and 0.34 (four s, 12H, $2Si(CH_3)_2$); 1.88–2.05 (m, 4H,

Table 5 Crystallographic data and refinement parameters for the structures **8a**, **8a′**, **8c** and **9a**

	8a	8a′	8c	9a
Molecular formula	$C_{12}H_{26}N_2O_4SSi_2$	$C_{12}H_{26}N_2O_4SSi_2$	$C_{10}H_{24}N_2O_4SSi_2$	$C_{12}H_{26}F_2N_2O_3SSi_2$
Formula weight	350.59	350.59	324.55	372.59
Crystal system	Orthorhombic	Monoclinic	Monoclinic	Orthorhombic
Space group	$P2_12_12_1$	$P2_1$	$P2_1/n$	$P2_12_12_1$
Flack parameter	0.027(18)	0.03(9)	—	0.016(13)
Z	8	2	4	8
a, Å	9.6000(5)	7.436(4)	15.1089(9)	13.0441(9)
b, Å	14.2422(7)	9.474(6)	6.6275(4)	15.9282(11)
c, Å	27.0844(14)	14.125(9)	16.4442(10)	18.2980(13)
α, °	90	90	90	90
β, °	90	104.082(9)	98.7620(10)	90
γ, °	90	90	90	90
V, Å^3	3703.1(3)	965.2(10)	1627.41(17)	3801.8(5)
ρ_{calc} (g cm^{-3})	1.258	1.206	1.325	1.302
μ, cm^{-1}	3.19	3.06	3.57	3.25
F(000)	1504	376	696	1584
$2\theta_{max}$, °	61.03	60.22	60.06	61.06
Reflections collected	50 072	10 584	30 094	65 941
Independent reflections (R_{int})	11 308 (0.0355)	5331 (0.00)	4740 (0.0311)	11 597 (0.0327)
Number of reflections with $I > 2\sigma(I)$	10 588	3228	3981	10 557
Parameters	389	195	178	411
R_1 [$I > 2\sigma(I)$]	0.0344	0.0579	0.0484	0.0266
wR_2 (all independent reflections)	0.0793	0.1168	0.1022	0.0698
GOF	1.071	1.000	1.034	1.084
ρ_{min}/ρ_{max} (e Å^{-3})	0.556/−0.323	0.873/−0.494	0.565/−0.358	0.381/−0.197

C^3H_2 and C^4H_2 Pro); 2.42 (s, 3H, $ArCH_3$); 2.95 and 3.14 (dd, 2H, NCH_2Si, $^3J_{HH}$ 15.0 Hz); 2.99 and 3.04 (dd, 2H, NCH_2Si, $^3J_{HH}$ 15.95 Hz); 3.39–3.46 and 3.50–3.57 (two m, 2H, C^5H_2 Pro); 4.87–4.92 (m, 1H, C^2H Pro); 7.28 and 7.79 (two d, 4H, Ar, $^3J_{HH}$ 8 Hz). ^{13}C NMR spectrum ($CDCl_3$, δ, ppm): –0.57 ÷ 0.00 (m, $2SiMe_2$); 21.47 (Me); 24.75 (^4C Pro); 30.89 (^3C Pro); 37.96 and 40.41 (two s, NCH_2Si); 48.09 (^5C Pro); 57.60 (C^2 Pro); 127.48 (C^2 and C^6 Ar), 129.30 (C^3 and C^5 Ar), 136.50 (C^1 Ar), 143.04 (C^4 Ar), 169.52 (C=O). ^{29}Si NMR spectrum ($CDCl_3$, δ, ppm): 7.9, 10.4.

2,2,6,6-Tetramethyl-4-(*N*-mesylsarcosinyl)-2,6-disilamorpholine (8c)

Prepared similar to **8a** from 0.83 g of **6c**. Yield 1.3 g (80%) with m.p. 151–153 °C (from heptane–benzene, 7 : 1). Found, %: C 37.28, H 7.24, N 8.64, S 9.51. $C_{10}H_{24}N_2O_4SSi_2$. Calculated, %: C 37.01, H 7.45, N 8.63, S 9.88. IR spectrum (KBr, ν, cm^{-1}): 1628 s (C=O), 1323 s, 1153 s (SO_2). ^1H NMR spectrum ($CDCl_3$, δ, ppm): 0.18 and 0.23 (two s, 12H, $2Si(CH_3)_2$); 2.79 and 3.06 (two s, 4H, NCH_2Si); 2.98 (s, 3H, NCH_3); 2.99 (s, 3H, SCH_3); 4.13 (s, 2H, NCH_2). ^{13}C NMR spectrum ($CDCl_3$, δ, ppm): –0.37 and −0.19 (two s, $2Si(CH_3)_2$); 35.44 (NMe); 37.95 and 39.70 (two s, NCH_2Si); 38.15 (SMe); 51.56 (NCC=O); 165.58 (C=O). ^{29}Si NMR spectrum ($CDCl_3$, δ, ppm): 8.3, 10.4.

N′,*N*′-Bis(dimethylfluorosilylmethyl)-*N*-mesyl-(*S*)-prolinamide (9a)

Boron trifluoride (0.36 g, 2.5 mmol) was added dropwise to a solution of **8a** (0.88 g, 2.5 mmol) in acetonitrile (5 mL). The reaction mixture was refluxed for 2 h, then evaporated in vacuum. The remaining oil was refluxed with benzene (15 mL), the precipitate was filtered out, and the solution was evaporated in vacuum. The residue was recrystallised from heptane to afford 0.76 g (82%) of **9a** with m.p. 100–101 °C. Found, %: C 34.61, H 6.88, N 7.86, S 8.92. $C_{10}H_{24}F_2N_2O_3SSi_2$. Calculated, %: C 34.66, H 6.98, N 8.08, S 9.25. IR spectrum (KBr, ν, cm^{-1}): 1610 s, 1505 w (C=O), 1319 s, 1134 s (SO_2). ^1H NMR spectrum ($CDCl_3$, δ, ppm): 0.22 and 0.31 (two s, 6H, $Si^V(CH_3)_2$); 0.41 and 0.46 (dd, 6H, $Si^{IV}(CH_3)_2$, $^3J_{HF}$ 7.67 Hz); 1.86–1.93, 2.03–2.18 and 2.28–2.36 (m, 4H, C^3H_2 and C^4H_2 Pro); 2.44 and 2.59 (dd, 2H, NCH_2Si^V, $^3J_{HH}$ 15.74 Hz); 2.98 (s, 3H, SCH_3); 3.00–3.05 and 3.25–3.30 (two m, 2H, NCH_2Si^{IV}); 3.44–3.5 and 3.58–3.63 (two m, 2H, C^5H_2 Pro); 4.75–4.77 (m, 1H, C^2H Pro). ^{13}C NMR spectrum ($CDCl_3$, δ, ppm): −1.9 ÷ −1.7 (m, $Si^{IV}CH_3$); 1.1–1.7 (m, Si^VCH_3); 24.95 (C^4 Pro); 30.93 (C^3 Pro); 39.23 (SC); 41.1 ÷ 41.5 (m, CH_2Si^V and CH_2Si^{IV}); 47.72 (C^5 Pro); 56.59 (C^2 Pro); 172.51 (C=O). ^{19}F NMR spectrum ($CDCl_3$, δ, ppm): −159.15; −121.88. ^{29}Si NMR spectrum ($CDCl_3$, δ, ppm): −15.5 (d, $^1J_{SiF}$ 252 Hz), 28.9 (d, $^1J_{SiF}$ 284 Hz). ^{29}Si NMR CP/MAS spectrum (δ, ppm): −37.2 (d, $^1J_{SiF}$ 880 Hz), 32.7 (d, $^1J_{SiF}$ 1024 Hz).

N′,*N*′-Bis(dimethylfluorosilylmethyl)-*N*-tosyl-(*S*)-prolinamide (9b)

Prepared similar to **9a** from 1.1 g of **8b**. Yield 0.9 g (80%) with m. p. 87–88 °C (from heptane). Found, %: C 48.23, H 6.80, N 6.15, S 7.20. $C_{18}H_{30}F_2N_2O_3SSi_2$. Calculated, %: C 48.18, H 6.74, N 6.24, S 7.15. IR spectrum (KBr, ν, cm^{-1}): 1602 s, 1515 w (C=O), 1336 s, 1151 s (SO_2). ^1H NMR spectrum ($CDCl_3$, δ, ppm): 0.18 and 0.22 (two s, 6H, $Si^V(CH_3)_2$); 0.41–0.44 (m, 6H, $Si^{IV}(CH_3)_2$); 1.83–1.93 and 2.05–2.16 (two m, 4H, C^3H_2 and C^4H_2 Pro); 2.43 and 2.51 (dd, 2H, NCH_2Si^V, $^3J_{HH}$ 15.74 Hz); 2.45 (s, 3H, $ArCH_3$); 3.04–3.08 and 3.52–3.59 (two m, 2H, NCH_2Si^{IV}); 3.35–3.4 and 3.46–3.52 (two m, 2H, C^5H_2 Pro); 4.78–4.81 (m, 1H, C^2H Pro), 7.32 (d, 2H, Ar, $^3J_{HH}$ 8.07 Hz), 7.75 (d, 2H, Ar, $^3J_{HH}$ 8.07 Hz). ^{13}C NMR spectrum ($CDCl_3$, δ, ppm): −1.92 ÷ −1.78 (m, $Si^{IV}CH_3$); 1.20–1.37 (m, Si^VCH_3); 21.46 (ArMe); 24.89 (C^4 Pro); 30.63 (C^3 Pro); 41.27 (d, CH_2Si^{IV}, $^3J_{CF}$ 16.69 Hz); 41.36–41.47 (m, CH_2Si^V); 48.24 (C^5 Pro); 55.45 (C^2 Pro); 127.31 (C^2 and C^6 Ar), 129.64 (C^3 and C^5 Ar), 135.89 (C^1 Ar), 143.74 (C^4 Ar); 172.39 (C=O). ^{19}F NMR spectrum ($CDCl_3$, δ, ppm): −159.47; −119.31. ^{29}Si NMR spectrum ($CDCl_3$, δ, ppm): −19.1 (d, $^1J_{SiF}$ 236 Hz), 28.1 (d, $^1J_{SiF}$ 276 Hz). ^{29}Si NMR CP/MAS spectrum (δ, ppm): −32.0 (d, $^1J_{SiF}$ 251 Hz), 30.7 (d, $^1J_{SiF}$ 292 Hz).

N′,*N*′-Bis(dimethylfluorosilylmethyl)-*N*-mesylsarcosinamide (9c)

Prepared similar to **9a** from 0.80 g of **8c**. Yield 0.73 g (85%) with m. p. 135–136 °C (from heptane). Found, %: C 34.61, H 6.88, N 7.86, S 8.92. $C_{10}H_{24}F_2N_2O_3SSi_2$. Calculated, %: C 34.66, H 6.98, N 8.08, S 9.25. IR spectrum (KBr, ν, cm^{-1}): 1610 s, 1505 w (C=O), 1319 s, 1134 s (SO_2). ^1H NMR spectrum ($CDCl_3$, δ, ppm): 0.30 (two s, 6H, $Si(CH_3)_2$); 0.39–0.43 (m, 6H, $Si^{IV}(CH_3)_2$); 2.56 and 3.05 (two s, 4H, NCH_2Si); 2.96 (s, 3H, NCH_3); 2.98 (s, 3H, SCH_3); 4.17 (s, 2H, NCH_2). ^{13}C NMR spectrum ($CDCl_3$, δ, ppm): −1.8 (d, $SiMe_2$, $^2J_{CF}$ 14.5 Hz), 1.2 (s, $SiMe_2$); 35.3 (NMe); 37.9 and 40.8 (two s, NCH_2Si); 41.4 (SMe); 49.7 (NCC=O); 168.6 (C=O). NMR ^{19}F spectrum ($CDCl_3$, δ, ppm): −159.15; −125.46. ^{29}Si NMR spectrum ($CDCl_3$, δ, ppm): −10.5 (d, $^1J_{SiF}$ 248 Hz), 29.2 (d, $^1J_{SiF}$ 287 Hz).

Single crystals suitable for X-ray diffraction analysis were obtained by recrystallisation from: orthorhombic **8a**—heptane/benzene 3 : 1; monoclinic **8a**′—ethanol; **8c**—heptane/benzene 7 : 1; **9a**—heptane. X-ray diffraction measurements were carried out using Bruker Smart 1000 CCD and Bruker Smart Apex II CCD diffractometers at 100 K. The frames were integrated using SMART and APEX2 program packages.[28] The correction for absorption was made using SADABS program.[29] The details of crystallographic data and experimental conditions are given in Table 5.

The structures were solved by the direct method by XS program[30] and refined by full-matrix least-squares technique against F^2 in the anisotropic–isotropic approximation using XL program.[30] Atom H20 in s was located from the difference Fourier maps and refined freely. All remaining hydrogen atoms were placed in geometrically calculated positions and refined in rigid body model ($U_{iso}(H) = 1.2U_{eq}(CH, CH_2)$, $U_{iso}(H) = 1.5U_{eq}(CH_3)$). The Flack parameter confirms (*S*)-configuration of the proline fragment. Preparation of graphic materials was performed using OLEX2 software package.[31] Crystallographic data for the structural analysis of **8a**, **8a**′, **8c** and **9a** have been deposited with the Cambridge Crystallographic Data Centre (CCDC nos 1059570–1059573).

Acknowledgements

This work was carried out as a part of the research activities of the Science and Education Centre for the Synthesis and Investigation of Biologically Active Compounds at the N. I. Pirogov Russian National Research Medical University and supported by the Russian Foundation for Basic Research (grants nos 16-03-00957, 16-33-60168 and 16-33-00956).

References

1 (*a*) C. Chuit, R. J. P. Corriu, C. Reye and J. C. Young, *Chem. Rev.*, 1993, **93**, 1371–1448; (*b*) D. Kost and I. Kalikhman, in *The Chemistry of Organic Silicon Compounds*, ed. Z. Rappoport and Y. Apeloig, Wiley, Chichester, U.K., 1998, vol. 2, pp. 1339–1445; (*c*) J. Wagler, U. Böhme and E. Kroke, in *Functional Molecular Silicon Compounds I: Regular Oxidation States*, ed. D. Scheschkewitz, Springer, 2014, pp. 29–105.

2 (*a*) V. V. Negrebetsky and Y. I. Baukov, *Russ. Chem. Bull.*, 1997, **46**, 1807–1831; (*b*) V. V. Negrebetsky, S. N. Tandura and Y. I. Baukov, *Russ. Chem. Rev.*, 2009, **78**, 21–51; (*c*) A. A. Nikolin and V. V. Negrebetsky, *Russ. Chem. Rev.*, 2014, **83**(9), 848–883.

3 A. Chandra, R. Sheker, Z. Chen, T. Hatanaka, T. Minami and Y. Hatanaka, *Organometallics*, 2013, **32**, 3575–3582; Y. Li, C. deKock, P. J. Smith, H. Guzgay, D. T. Hendricks, K. Naran, V. Mizrahi, D. F. Warner, K. Chibale and G. S. Smith, *Organometallics*, 2013, **32**, 141–150; T. Baramov, K. Keijzer, E. Irran, E. Mösker, M.-H. Baik and R. Süssmuth, *Chem.–Eur. J.*, 2013, **19**, 10536–10542; Y. Tokoro, H. Yeo, K. Tanaka and Y. Chujo, *Polym. Chem.*, 2013, **4**, 5237–5242; Y. Hatanaka, S. Okada, T. Minami, M. Goto and K. Shimada, *Organometallics*, 2005, **24**, 1053–1055.

4 E. Lukevics and L. Ignatovich, in *Metallotherapeutic Drugs and Metal-Based Diagnostic Agents*, ed. M. Gielen and T. E. R. Tiekink, Wiley, 2005, pp. 83–108.

5 (*a*) K. Junold, J. A. Baus, C. Burschka, D. Auerhammer and R. Tacke, *Chem.–Eur. J.*, 2012, **18**, 16288–16291; (*b*) K. Junold, J. A. Baus, C. Burschka, C. F. Guerra, F. M. Bickehaupt and R. Tacke, *Chem.–Eur. J.*, 2014, **20**, 12411–112415; (*c*) S. Metz, C. Burschka, D. Platte and R. Tacke, *Angew. Chem., Int. Ed.*, 2007, **46**, 7006–7009; (*d*) D. Troegel, C. Burschka, S. Riedel, M. Kaupp and R. Tacke, *Angew. Chem., Int. Ed.*, 2007, **46**, 7001–7005; (*e*) R. Tacke, C. Burschka, I. Richter, B. Wagner and R. Willeke, *J. Am. Chem. Soc.*, 2000, **122**, 8480–8485.

6 (*a*) R. W. Hillyard Jr, M. C. Ryan and C. H. Yoder, *J. Organomet. Chem.*, 1978, **153**(3), 369–377; (*b*) K. D. Onan, A. T. McPhail, C. H. Yoder and R. W. Hillyard Jr, *Chem. Commun.*, 1978, **5**, 209–210; (*c*) A. R. Bassindale and M. Borbaruah, *J. Chem. Soc., Chem. Commun.*, 1993, 352–353; (*d*) A. G. Shipov, E. P. Kramarova, E. A. Mamaeva, O. A. Zamyshlyaeva, V. V. Negrebetsky, Y. E. Ovchinnikov, S. A. Pogozhikh, A. R. Bassindale, P. G. Taylor and Y. I. Baukov, *J. Organomet. Chem.*, 2001, **620**, 139–145; (*e*) A. A. Korlyukov, K. A. Lyssenko, M. Y. Antipin, A. G. Shipov, O. A. Zamyshlyaeva, E. P. Kramarova, V. V. Negrebetsky, S. A. Pogozhikh, Y. E. Ovchinnikov and Y. I. Baukov, *Russ. Chem. Bull.*, 2004, **53**(9), 1924–1931.

7 (*a*) A. A. Nikolin, E. P. Kramarova, A. G. Shipov, Y. I. Baukov, V. V. Negrebetsky, A. A. Korlyukov, D. E. Arkhipov, A. Bowden, S. Y. Bylikin, A. R. Bassindale and P. G. Taylor, *Organometallics*, 2012, **31**(14), 4988–4997; (*b*) A. A. Nikolin, O. V. Kuznetsova, D. E. Arkhipov, E. P. Kramarova, A. G. Shipov, A. N. Egorochkin, A. A. Korlyukov, Y. I. Baukov and V. V. Negrebetsky, *Russ. Chem. Bull.*, 2013, **8**, 1892–1899.

8 (*a*) E. P. Kramarova, V. V. Negrebetsky, A. G. Shipov and Y. I. Baukov, *Russ. J. Gen. Chem.*, 1994, **64**; *Zh. Obshch. Khim*, 1994, **64**, 1222–1223; (*b*) Y. I. Baukov, A. G. Shipov, E. P. Kramarova, E. A. Mamaeva, O. A. Zamyshlyaeva, N. A. Anisimova and V. V. Negrebetsky, *Russ. J. Org. Chem.*, 1996, **32**, 1259–1271.

9 Y. I. Baukov, E. P. Kramarova, A. G. Shipov, G. I. Oleneva, O. B. Artamkina, A. I. Albanov, M. G. Voronkov and V. A. Pestunovich, *J. Gen. Chem. USSR*, 1989, **59**; *Zh. Obshch. Khim*, 1989, **59**, 127–145.

10 A. A. Nikolin, D. E. Arkhipov, A. G. Shipov, E. P. Kramarova, N. A. Koval'chuk, A. A. Korlyukov, V. V. Negrebetsky, Y. I. Baukov, A. R. Bassindale, P. G. Taylor, A. Bowden and S. Y. Bylikin, *Chem. Heterocycl. Compd.*, 2012, **47**(12), 1565–1583.

11 E. P. Doronina, V. F. Sidorkin and N. F. Lazareva, *J. Phys. Chem. A*, 2015, **119**, 3663–3673.

12 N. N. Chipanina, T. N. Aksamentova, M. G. Voronkov and V. K. Turchaninov, *J. Struct. Chem.*, 2006, **46**, 1066–1070ss.

13 V. V. Negrebetsky, A. G. Shipov, E. P. Kramarova, V. V. Negrebetsky and Y. I. Baukov, *J. Organomet. Chem.*, 1997, **530**, 1–12.

14 O. B. Bannikova, A thesis for the degree of candidate of chemical Sciences, The Institute of Organic Chemistry, Russian Academy of Science, Irkutsk, 1986, p. 20.

15 (*a*) A. Lends, E. Olszewska, S. Belyakov, N. Erchak and E. Liepinsh, *Heteroat. Chem.*, 2015, **26**, 12–28; (*b*) R. Tacke, J. Becht, O. Dannappel, R. Ahlrichs, R. Schneider, W. S. Sheldrick, J. Hahn and F. Kiesgen, *Organometallics*, 1996, **15**, 2060–2077; (*c*) O. Girdhberg, I. Kalikhman, D. Stalke, B. Walfort and D. Kost, *J. Mol. Struct.*, 2003, **661–662**, 259–264; (*d*) V. V. Negrebetsky, S. Y. Bylikin, A. G. Shipov, Y. I. Baukov, A. R. Bassindale and P. G. Taylor, *J. Organomet. Chem.*, 2003, **678**, 39–47.

16 F. H. Allen, *Acta Crystallogr., Sect. B: Struct. Sci.*, 2002, **58**, 380.

17 V. F. Sidorkin, E. F. Belogolova and V. A. Pestunovich, *Chem.–Eur. J.*, 2006, **12**, 2021–2031.

18 M. J. Frisch, G. W. Trucks, H. B. Schlegel, G. E. Scuseria, M. A. Robb, J. R. Cheeseman, J. Montgomery, T. Vreven, K. N. Kudin, J. C. Burant, J. M. Millam, S. S. Iyengar, J. Tomasi, V. Barone, B. Mennucci, M. Cossi, G. Scalmani, N. Rega, G. A. Petersson, H. Nakatsuji, M. Hada, M. Ehara, K. Toyota, R. Fukuda, J. Hasegawa, M. Ishida, T. Nakajima, Y. Honda, O. Kitao, H. Nakai, M. Klene, X. Li, J. E. Knox,

H. P. Hratchian, J. B. Cross, V. Bakken, C. Adamo, J. Jaramillo, R. Gomperts, R. E. Stratmann, O. Yazyev, A. J. Austin, R. Cammi, C. Pomelli, J. W. Ochterski, P. Y. Ayala, K. Morokuma, G. A. Voth, P. Salvador, J. J. Dannenberg, V. G. Zakrzewski, S. Dapprich, A. D. Daniels, M. C. Strain, O. Farkas, D. K. Malick, A. D. Rabuck, K. Raghavachari, J. B. Foresman, J. V. Ortiz, Q. Cui, A. G. Baboul, S. Clifford, J. Cioslowski, B. B. Stefanov, G. Liu, A. Liashenko, P. Piskorz, I. Komaromi, R. L. Martin, D. J. Fox, T. Keith, M. A. Al-Laham, C. Y. Peng, A. Nanayakkara, M. Challacombe, P. M. W. Gill, B. Johnson, W. Chen, M. W. Wong, C. Gonzalez and J. A. Pople, *Gaussian 03, C.01*.

19 G. A. Zhurko and D. A. Zhurko, *Chemcraft Program, Academic version 1.7*, 2011.

20 S. Kim, P. A. Thiessen, E. E. Bolton, J. Chen, G. Fu, A. Gindulyte, L. Han, J. He, S. He, B. A. Shoemaker, J. Wang, B. Yu, J. Zhang and S. H. Bryant, *Nucleic Acids Res.*, 2016, **44**, D1202–D1213, DOI: 10.1093/nar/gkv951.

21 D. A. Filimonov, A. A. Lagunin, T. A. Gloriozova, A. V. Rudik, D. S. Druzhilovskii, P. V. Pogodin and V. V. Poroikov, *Chem. Heterocycl. Compd.*, 2014, **50**, 444–457.

22 A. Lagunin, A. Zakharov, D. Filimonov and V. Poroikov, *Mol. Inf*, 2011, **30**, 241–250.

23 *Pulse methods in 1D and 2 D liquid-phase NMR*, ed. W. S. Brey, Academic Press, New York, 1988, p. 561.

24 A. L. van Geet, *Analyt. Chem.*, 1970, **42**, 679–680.

25 G. Haegele, R. Fuhler and T. Lenzen, *Comp. Chem.*, 1995, **19**, 277–282.

26 G. Binsch, in *Dynamic Nuclear Magnetic Resonance Spectroscopy*, ed. L. Jackman and M. F. A. Cotton, Academic Press, New York, 1975, p. 45.

27 J. Tesse, *Bull. Soc. Chim. Fr.*, 1973, 787–793.

28 *APEX2, SMART, SAINT, SAINT-Plus*, Bruker AXS Inc., Madison, Wisconsin, USA, 2007.

29 *SADABS*, Bruker AXS Inc., Madison, Wisconsin, USA, 2001.

30 G. M. Sheldrick, Crystal structure refinement with SHELXL, *Acta Crystallogr., Sect. C: Struct. Chem.*, 2015, **71**, 3–8.

31 O. V. Dolomanov, L. J. Bourhis, R. J. Gildea, J. A. K. Howard and H. Puschmann, *J. Appl. Crystallogr.*, 2009, **42**, 339–341.